

Development of a polarized solid ^7LiD target system for spin-dependent EMC effect experiments with CLAS12

T. Kageya* and **D. Akers, J. Brock, C. Carlin, J. Creel, G. Dezern, P. Dobrenz, C. Flanagan, D. Griffith, M. Hoegerl, P. Hood, C.D. Keith, S. Madlock, B. Mastracci, J. Maxwell, D. Meekins, M. Poelker, E. Pozdeyev, X. Wei, D. Williams**

*Thomas Jefferson National Accelerator Facility,
12000 Jefferson Ave., Newport News, VA 23606, USA*

E-mail: kageya@jlab.org

In order to try to settle the question of the origin of the EMC effect, experiments will be performed to study polarized EMC effects at Hall B at Thomas Jefferson National Accelerator Facility (JLab). They will use longitudinally polarized 11 GeV electron beams and longitudinally polarized ^7LiD and NH_3 targets with CLAS12 detectors. JLab target and collaborating groups (Hall B group, engineering and accelerator divisions) are preparing an irradiation beam line, designing and constructing irradiation and DNP (Dynamic Nuclear Polarization) polarizing cryostats.

*20th International Workshop on Polarized Sources, Targets and Polarimetry,
22-27 September 2024
Jefferson Lab, Newport News, USA*

*Speaker

1. Introduction

The quark's distributions which can be accessed by DIS (Deep Inelastic Scattering) have been found to be different for free (least bound) and bound nucleons. This has been called EMC (European Muon Collaboration) effect and various theoretical approaches have been taken to explain and interpret them without success. Experiments will be performed to study polarized EMC effect at Hall B at JLab to try to settle the question of the origin of the EMC effect [1]. They will use longitudinally polarized 11 GeV electron beams and longitudinally polarized ^7LiD and NH_3 targets with CLAS12 detectors. The polarized quark distributions for a bound proton can be obtained via proton in polarized ^7Li on ^7LiD while those for a free proton via three polarized hydrogens in NH_3 . The structure of low mass nuclei like ^7Li and that of their spins are rather well known. JLab target and collaborating groups (Hall B group, engineering and accelerator divisions) are preparing an irradiation beam line, designing and constructing irradiation and DNP (Dynamic Nuclear Polarization) polarizing cryostats [2]. All of these equipments are located at JLab on-site which allow us to control and optimize an irradiation temperature and dose, to measure a polarization and build-up time for irradiated samples consecutively and to obtain more understanding of free radical conditions after an irradiation, damage by beam and annealing via ESR and IR spectroscopy [2]. From the past records of data by other groups, we will discuss the expected polarization and build-up time for ^7LiD , its irradiation conditions and possible options.

2. EMC effect

2.1 Unpolarized EMC effect

The quark distribution accessed via DIS can be the same or similar for light and heavy nuclei. If we take ratios of the unpolarized structure function F_2 of heavy nucleus to that of the light nucleus (in this case the deuteron) considering the number of nucleons as a function of Bjorken x , they have been observed to significantly deviate from unity depending on x . In other words, the nuclear structure functions differ significantly from the sum of those of proton and neutron. The ratio is defined as

$$R_A = \frac{F_{2A}}{ZF_{2p} + (A - Z)F_{2n}} \quad (1)$$

where F_{2A} , F_{2p} and F_{2n} are unpolarized structure functions F_2 for the nucleus A, free (lightly bound) proton and neutron [3], respectively.

The effect was observed by EMC (European Muon Collaboration) for the first time and that is why it has been called the EMC effect. The experiment was performed with muon beams at CERN in the 1970's and 80's. There is no clear explanations and interpretations for this effect and different theoretical approaches have been developed in different x regions. The effect has been studied from heavy nuclei like iron, calcium and copper (an example of plots as shown in Figure 1) [4] to lighter ones like ^9Be and ^4He (shown in Figure 2) [5] by different experiments. No data were taken for the EMC effect of ^7Li whose atomic number is between ^4He and ^9Be , but it is expected that the effect will be observed for ^7Li .

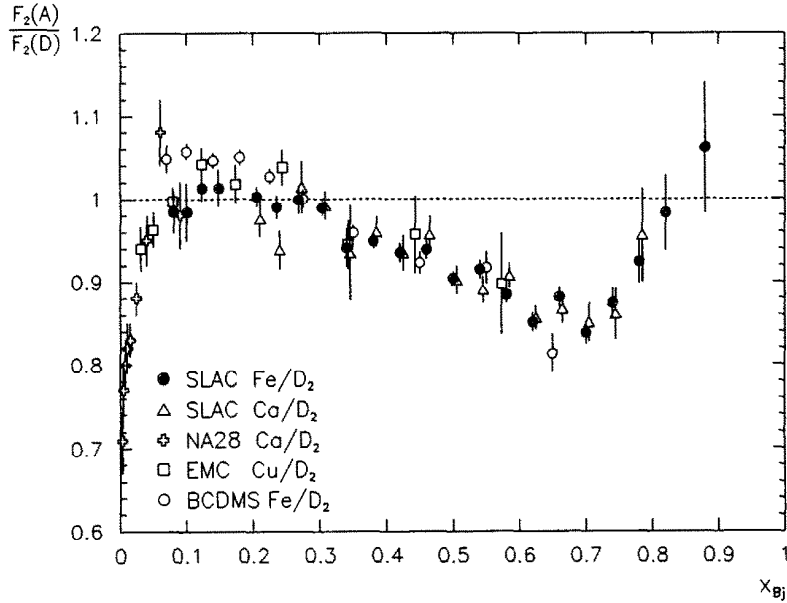


Figure 1: An example of unpolarized EMC effects observed. Ratios of unpolarized structure function F_2 for heavy nuclei (iron, copper and calcium) to those for light nucleus (deuteron) are plotted as a function of x_{BJ} [4].

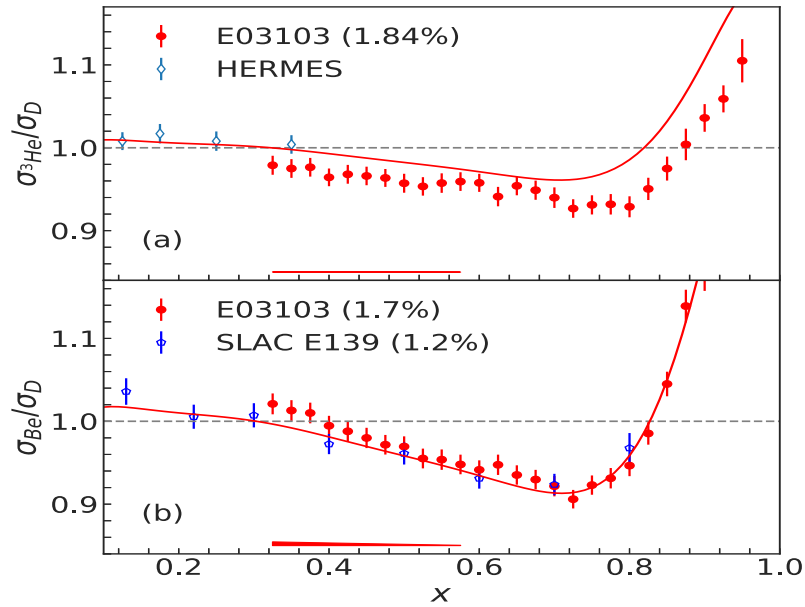


Figure 2: An example of unpolarized EMC effects observed for lighter nuclei. Ratios of unpolarized structure function F_2 for nuclei (^9Be and ^4He) to those for light nucleus (deuteron) are plotted as a function of x_{BJ} [5].

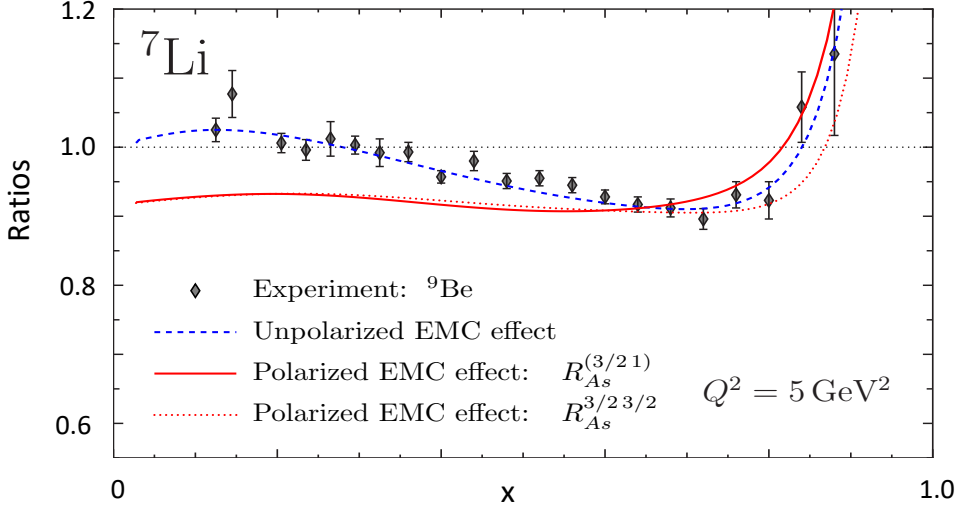


Figure 3: Theoretical predictions for polarized EMC effects on ^7Li are shown with red curves [3] as a function of x , while both black plots and blue dashed curve are unpolarized EMC effect on ^9Be from experimental data [6] and predictions [7], respectively.

2.2 Spin-dependent EMC effect

By comparing spin-dependent structure functions g_1 for bound with unbound protons, we will be able to explore spin-dependent EMC effects which may be more enhanced than unpolarized ones according to some theoretical predictions and may allow to settle the question of the origin of the EMC effect at Jefferson Lab. [1]. In Figure 3, some predictions for the polarized EMC effect in ^7Li are shown on the red curves (the solid and dotted ones are from different definitions of the ratios) [3], while both the black plots and the blue dashed curve are the effect of the unpolarized EMC in ^9Be from experimental data taken at SLAC [6] and theoretical prediction [7], respectively.

3. Advantages of using ^7LiD and NH_3

3.1 Structure of ^7Li

The structure of light nuclei is well known. With the shell model [8] and more recently according to Quantum Monte Carlo calculations, the bound proton in the $P_{3/2}$ shell carries about 87 % of the ^7Li spin, the two $P_{3/2}$ neutrons about - 0.4 % and the $S_{1/2}$ nucleons carry zero [3] [7] [9] (Figure 4). Three hydrogens in NH_3 are used as free polarized protons.

3.2 Packing fraction

Commercially available ^7LiD has a shape of powder or chunk. One of possible shapes, we are considering for the ^7LiD target is a series of thin, solid disks. Disks can be better fit to the target cell reducing a volume of liquid ^4He in the cell and increasing the ratio of the volume of the

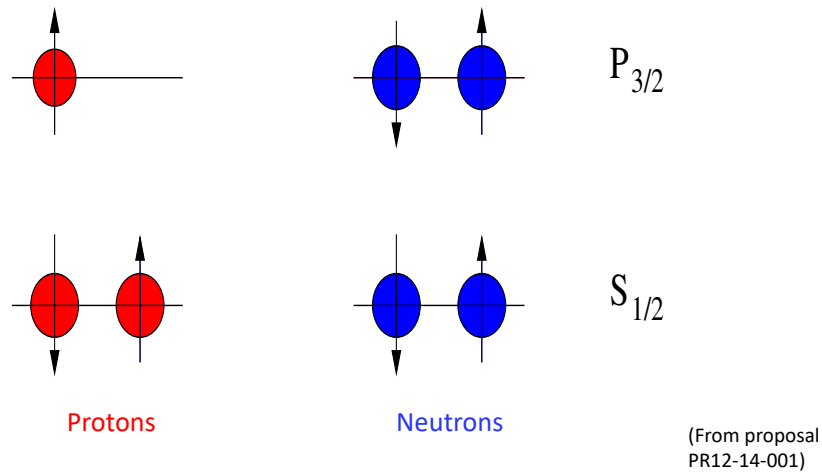


Figure 4: ${}^7\text{Li}$ consists of $S_{1/2}$ four nucleons, two $P_{3/2}$ neutrons and one bound $P_{3/2}$ proton from the shell model [8].

target material to that of the cell compared to other target materials that have shapes of a couple of mm in size. The CLAS12 detectors have enough z-vertex (beam direction) resolutions to separate events originating at target region from others. We can obtain the better estimation and control of this packing fraction than for other target materials, NH_3 , ND_3 and butanol whose packing fraction is not greater than 0.6. We are requesting a service work to Y12 in Oak Ridge to press the ${}^7\text{LiD}$ material to produce a disk of 20 mm diameter and 2 mm thickness. New NH_3 material will be supplied by a group of University of New Hampshire in collaboration.

3.3 Target polarization

There is not much data for ${}^7\text{Li}$ in ${}^7\text{LiD}$. The only data from four groups at PSI [10], Bonn [11], SLAC [12] and COMPASS [13] show about 90 % (0.3 K and 2.5 T), -37 % (1 K and 2.5 T), 64 % (1 K and 5 T) and 90 % (dilution fridge temp. and 2.5 T) polarizations for ${}^7\text{Li}$, respectively. The data were taken for samples to intend to polarize ${}^6\text{LiD}$ which contain 5 % (PSI [10], Bonn [11] and COMPASS [13]) and 15 % (SLAC [12]) of ${}^7\text{Li}$ in Li. This is the first time to intend to polarize ${}^7\text{LiD}$ whose ${}^7\text{Li}$ ratio is more than 92 % in Li (detailed numbers for isotopic and chemical impurities are described in Section 3.7). From the above data, as high as ~ 64 % of polarization for ${}^7\text{Li}$ in ${}^7\text{LiD}$ could be expected at 1 K and 5 T (see Table 1 and discussion at Section 5.2).

For NH_3 , H polarization as high as 90 % with its average of more than 70 % during experiments is expected as in the past by different experiments (an example is in [14]) including RGC experiments whose systems will be used for this experiment [15].

3.4 Dilution factor

A ratio of the number of polarized bound proton in ${}^7\text{Li}$ to that of total nucleons in ${}^7\text{LiD}$ is one to nine which is 0.11. For NH_3 , a ratio of the number of free protons to that of total nucleons is three to seventeen, which is 0.17. These are acceptable for this experiment. As other possible candidates of stable nuclei for polarized EMC effect, we may pick up ${}^{11}\text{B}$ (5p, 6n), ${}^{15}\text{N}$ (7p, 8n), ${}^{19}\text{F}$ (9p, 10n) and ${}^{27}\text{Al}$ (13p, 14n) based on their reasonable natural abundance ratios. The dilution factors are smaller for heavier nuclei and ${}^7\text{LiD}$ can be one of the best candidates.

3.5 Radiation resistance

NH_3 , ND_3 and ${}^6\text{LiD}$ have been used as highly polarized targets by different experiments showing reasonable radiation resistance to high currents of electron beams. In this case, radiation resistance means how pre-irradiated (at high temperature with no magnetic field) target material can hold the polarization on high energy beam at low temperature during scattering experiments (at 1 Kelvin with a field of 5 Tesla in our case). Structures of paramagnetic centers produced by primary irradiation performed at high temperature (for example, at liquid argon temperature of 87 K for NH_3 and ND_3 or at 180 K for ${}^6\text{LiD}$ targets) and by additional irradiation at low temperature like 1 K in our case are different [11]. The two procedures with these conditions are treated as different ones.

There is no data for radiation damages to ${}^7\text{LiD}$. We can pick up some observations of radiation damages for ${}^7\text{LiH}$ and ${}^6\text{LiD}$ as below.

35

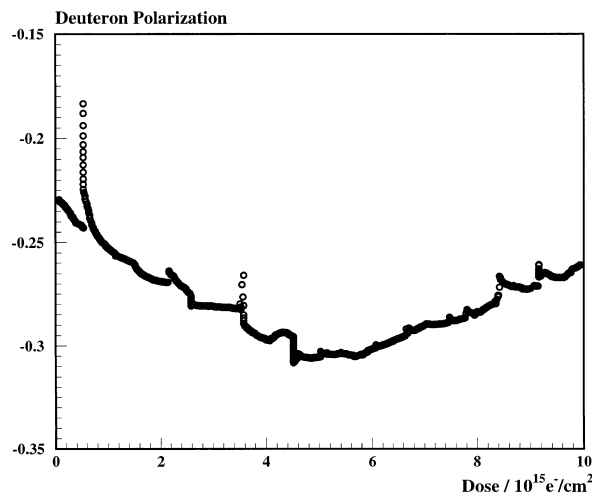


Figure 5: An example of radiation damages to ${}^6\text{LiD}$ target material. The plots are negatively polarized deuteron polarizations as a function of dose of electron measured at around 1 K during E155 experiments at SLAC in addition to the primary dose of 2×10^{17} (e/cm^2) [12].

The Bonn group showed that proton polarization, 11.5 % in ${}^7\text{LiH}$ increased to 14.5 % with

additional dose of 10^{15} (e/cm^2) at low temperature to the initial dose of 10^{17} (e/cm^2) and the polarization build-up time decreased from 50 to 8 min.

Up to additional dose of 5×10^{15} (e/cm^2), build-up time remained constant and no reduction in the maximum polarization was observed according to the group [11]. This suggests that ^7LiH has a strong radiation resistance to electron beam.

As an example of ^6LiD radiation damage shown in Figure 5, the data plots show deuteron polarizations in ^6LiD versus accumulated dose of high energy electron beams at 1 K [12]. The negative polarization increased until the ^6LiD target accumulated a dose of 5×10^{15} (e/cm^2) in addition to the primary dose of 2×10^{17} (e/cm^2) and started decreasing after that due to radiation damages to ^6LiD material. According to the article, ^6LiD has about five times larger radiation resistance than ND_3 [12]. The ^6Li polarizations are expected to behave as those of D in ^6LiD , because the equal spin temperature assumption can be applied to these two nuclei (see Section 5.1).

Similar high radiation resistance is expected for ^7LiD .

3.6 This RGG experiment and its setup

The same polarized target setup, ^4He evaporation cryostat including NMR and microwave system [15–18], which showed excellent performances for CLAS12 RGC (Run Group C) experiments in 2022 and 2023 at Hall B, will be used for this RGG experiment. A side view of the setup of polarized target system at Hall B beam line is shown in Figure 6 [15]. Tools to extract hydrogen and deuteron polarizations in NH_3 and to correct background scattering contributions from the nitrogen in them have been well established via semi-inclusive and elastic scattering on the data.

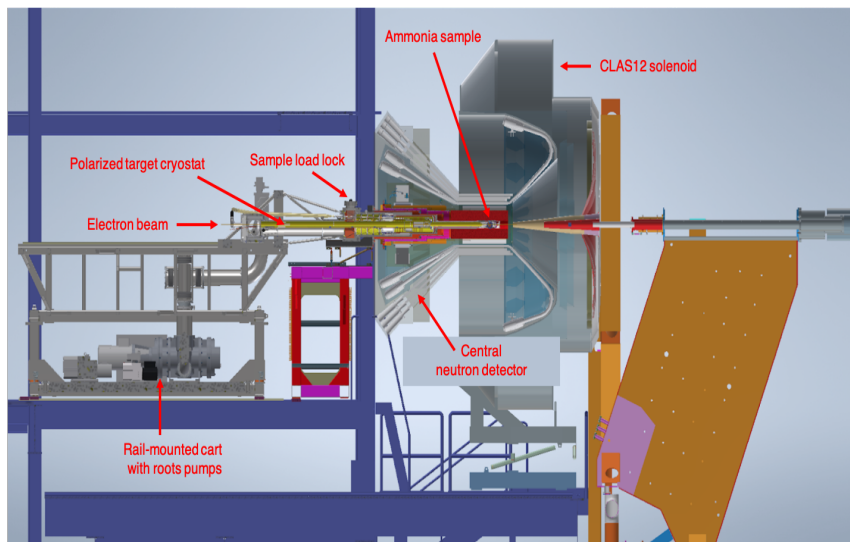


Figure 6: Side view of RGC experimental setup and beam line at Hall B. The horizontal ^4He evaporation cryostat is inserted into the center of CLAS12 detectors and solenoid magnet [15].

3.7 Impurities

The commercially available ^7LiD contains isotopic impurities of ^6Li ($\sim 7\%$) and H ($\sim 2\%$) [19] and chemical impurities (up to 5%), primarily $^7\text{LiOX}$, $^7\text{LiOX-X}_2\text{O}$, $^7\text{Li}_2\text{CO}_3$ (X: D or/and H) and others. About 5% of chemical impurities were observed by an LLNL group for commercially available ^7LiH and they are $^7\text{LiOH}$, $^7\text{LiOH-H}_2\text{O}$, $^7\text{Li}_2\text{CO}_3$ and others [20]. One of the commercial companies shows 3% of chemical impurities for LiD on their web-site [19]. Similar impurities are possibly produced during production, handling and storage processes for these two isotopes, ^7LiD and ^7LiH . Contributions of these impurities to the spin dependent structure functions should be considered and corrected on the data analysis procedures.

4. Irradiation of ^7LiD and NH_3

We plan to irradiate ^7LiD and NH_3 to produce necessary paramagnetic centers for DNP using low energy electron beams from the injector of JLab CEBAF (Continuous Electron Beam Accelerator Facility) prior to this RGG experiment. The beam energy and its current are around 10 MeV and an order of $10\ \mu\text{A}$, respectively. The beam line facilities have been and will be setup at the injection line and consist of magnets to raster beam vertically, beam position monitor, irradiation cryostat, Faraday cup and beam dump (Figure 7). We have been designing and constructing an irradiation cryostat to supply paramagnetic centers to ^7LiD and NH_3 with an order of $10^{17}\ (\text{e}^-/\text{cm}^2)$ (Figure 8) [2]. This variable temperature cryostat is cooled by liquid and some gas ^4He supplied from JLab's central Helium liquefies and can be set up to operate at various temperature ranges from $\sim 3\text{ K}$ to 200 K for different irradiation conditions (to be discussed in Section 5). We plan to operate this cryostat not only for primary irradiation at higher temperature like at 180 K and but for

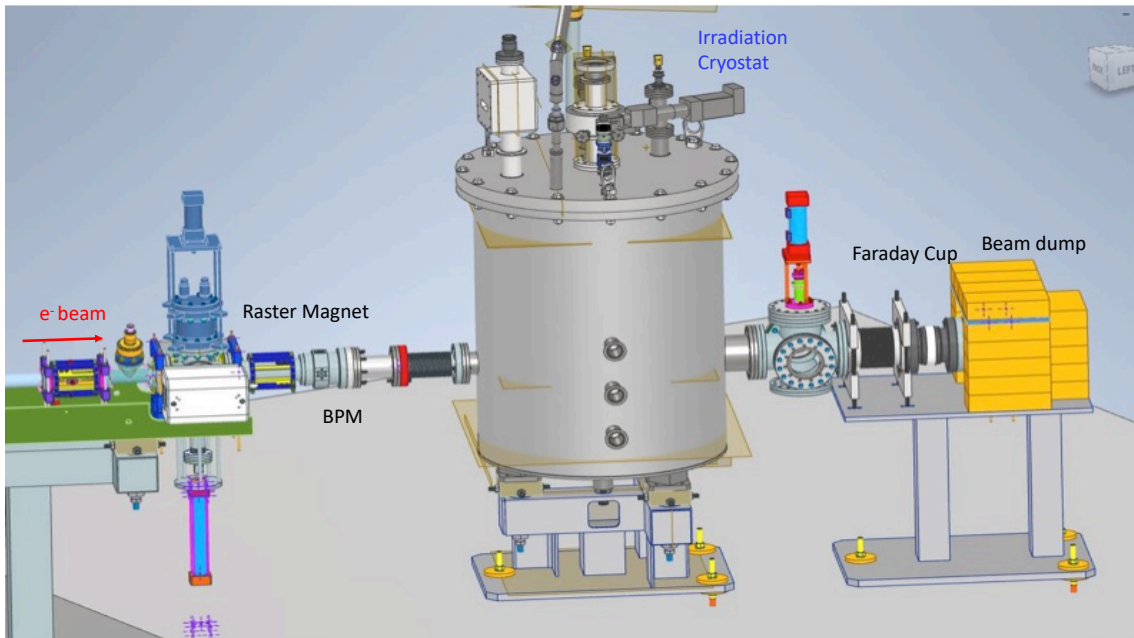


Figure 7: Side view of injector beam line for irradiation at JLab SEBAF. Consists of raster magnet, beam position monitor, irradiation cryostat, Faraday cup and beam dump.

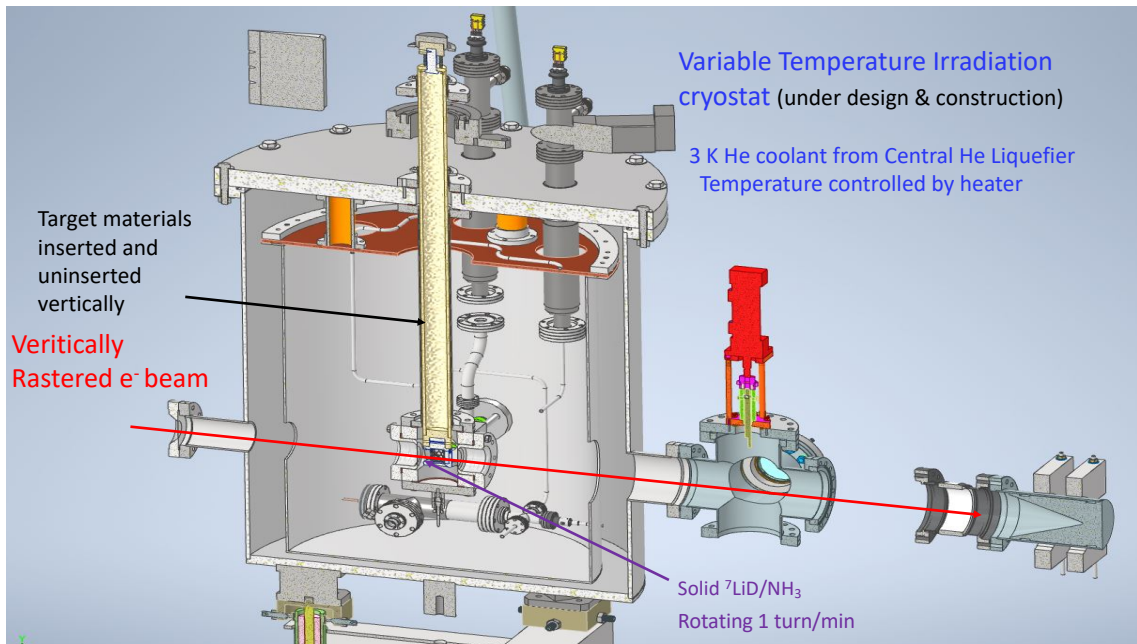


Figure 8: Detailed structure of irradiation cryostat. Vertically rastered electron beams will be exposed into target holder which is located on the bottom of inner fiberglass tube rotating once a minute with respect to the vertical axis [2].

additional irradiation at lower temperature of ~ 3 K. Used ${}^4\text{He}$ gas will be sent back to the supply facility for reuse. Target material container attached to the bottom of the inner fiberglass tube is inserted vertically into/from the cryostat through a central stainless steel tube. The inner tube rotates once per minute with respect to its vertical axis to expose the beam to the target homogeneously during the irradiation.

5. Dynamic Polarization of Lithium Hydride and Deuteride

For ${}^7\text{LiD}$, since there are very limited data, it is valuable to check data from ${}^7\text{LiH}$ and ${}^6\text{LiD}$ which consist of isotopes and their data are expected to show similar behaviors as ${}^7\text{LiD}$ which are seen in this Section. This work does not cover all of past results and picks up a part of them which are essentially useful. The higher polarization and shorter polarization build-up time are required when we install the targets prior to the experiments. During experiments every three days or so, the target polarization direction will be reversed with changing microwave frequency and we may anneal the targets when we observe radiation damages on them. Reasonably rapid obtaining thermal equilibrium signal for calibration of the polarization is also required. In rebuilding the polarization, a shorter build-up time after either of the aboves can reduce the loss of beam time. Definition of polarization build-up time is not consistent with amongst all authors below.

It is useful to apply and check the equal spin temperature (EST) assumption to ${}^7\text{Li}$, ${}^6\text{Li}$, H and D to understand their polarizations in ${}^7\text{LiD}$, ${}^7\text{LiH}$ and ${}^6\text{LiD}$ for the discussions in this work. For example, some data show only D (H) polarization instead of that of ${}^6\text{Li}$ (${}^7\text{Li}$) in ${}^6\text{LiD}$ (${}^7\text{LiH}$) which can be estimated from D (H) polarization, if EST assumption can be applied.

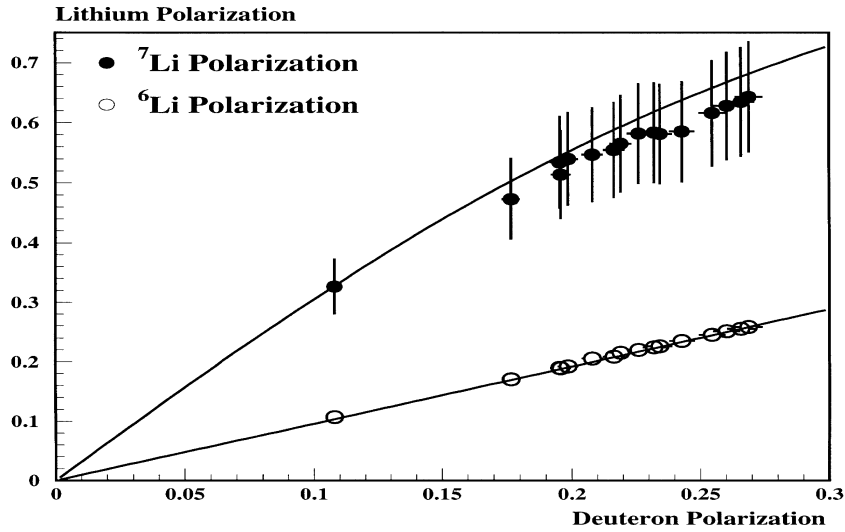


Figure 9: ${}^7\text{Li}$ (filled circles) and ${}^6\text{Li}$ (open circles) polarizations plotted as a function of D polarizations for ${}^6\text{LiD}$ sample measured at 1 K and 5 T by SLAC group for the dose of 3.7×10^{17} (e^-/cm^2). About 5 % of ${}^7\text{Li}$ was mixed in ${}^6\text{Li}$ for the sample. Two curves based on the EST assumption agree with measured data [12].

5.1 Equal spin temperature (EST)

The Bonn group measured polarizations of ${}^7\text{Li}$ and D in ${}^6\text{LiD}$ at 1 K and 2.5 Tesla and observed that the EST assumption can be applied to ${}^7\text{Li}$ and D [11], where about 15 % of ${}^7\text{Li}$ was mixed in ${}^6\text{Li}$ in ${}^6\text{LiD}$ material.

The SLAC group measured ${}^7\text{Li}$ ($\sim 5\%$ of ${}^7\text{Li}$ mixed in ${}^6\text{Li}$), ${}^6\text{Li}$ and D polarizations on the same ${}^6\text{LiD}$ target sample [12] at 1 K and 5 T. In Figure 9, ${}^7\text{Li}$ (filled circles) and ${}^6\text{Li}$ (open circles) polarizations are plotted as a function of D polarizations. The curves based on the assumption of EST between ${}^7\text{Li}$ and D, and ${}^6\text{Li}$ and D agree with data.

The COMPASS group confirmed the application of EST assumption to polarizations of ${}^7\text{Li}$, ${}^6\text{Li}$ and D for ${}^6\text{LiD}$ sample at dilution fridge temperature (~ 0.3 K) and 2.5 T [13]. About 5 % of ${}^7\text{Li}$ was mixed in ${}^6\text{Li}$ for the sample.

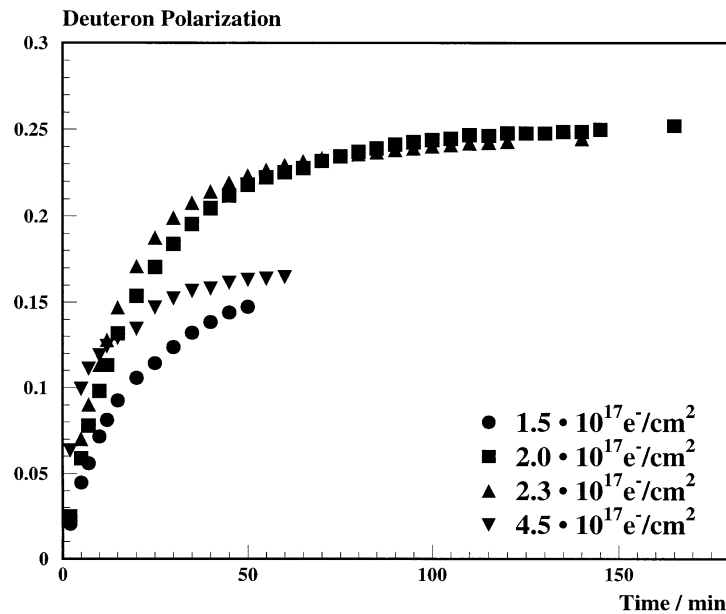
5.2 ${}^7\text{Li}$ polarization in ${}^7\text{LiD}$

The only data found for ${}^7\text{Li}$ in ${}^7\text{LiD}$ are shown in Table 1, although data were taken for ${}^7\text{Li}$ which was in ${}^6\text{Li}$ of about 5 % (PSI [10], SLAC [12] and COMPASS [13]) and 15 % (Bonn [11]). The only limited data from the SLAC group with our experimental conditions, at 1 K and 5 T, show as high as 64 % of ${}^7\text{Li}$ polarization in Figure 9. This is the first time to polarize ${}^7\text{LiD}$ whose ${}^7\text{Li}$ component (93 %) is higher than ${}^6\text{Li}$ (7 %) which may be challenging.

The description for build-up time has not been found for ${}^7\text{LiD}$. The SLAC group shows in Figure 10, deuteron polarization build-up behavior for ${}^6\text{LiD}$ target with different irradiation doses [12]. From this Figure, for the sample of dose of 2.0×10^{17} (e^-/cm^2) (filled square), at one

Table 1: Past records of irradiation conditions, obtained polarization for ^7Li in ^7LiD with their measurement conditions where ^7Li was in ^6Li with 5 % (PSI, SLAC and COMPASS) or 15 % (Bonn).

Group	T_{Ir} (K)	E_e^- (MeV)	Dose $\times 10^{17}$ (e^-/cm^2)	$P_{^7\text{Li}}$ (%)	P_D (%)	T(K)	B (Tesla)	Year
PSI [10]	180	3	2	90	51	0.2-0.4	2.5	1990
Bonn [11]	180	20	1	-37	-11	1	2.5	1995
SLAC [12]	180 ± 3	30	3.7	64 ± 9	26	1	5	1999
COMPASS [13]	190 ± 1	20	2	90	50	DF (~ 0.3 K)	2.5	2003


Figure 10: Deuteron polarization build-up behaviors for ^6LiD target with different irradiation doses prior to SLAC E155 experiments [12].

hour, about 22 % D polarization was obtained which corresponds to about 55 % ^7Li polarization according to EST. Relations between D and ^7Li polarizations based on EST can be seen in Figure 9.

From above, about 55 % ^7Li polarization is expected with build-up time of one hour for the sample dose of 2.0×10^{17} (e^-/cm^2).

5.3 ^7Li and H polarizations in ^7LiH

Table 2 shows past records of irradiation conditions, polarization, and build-up time for ^7Li in ^7LiH with their DNP conditions.

The Saclay group started irradiating at ≥ 87 K (liquid argon temperature, see caption of Table 2) [21] [22]. At 77 K (liquid nitrogen temperature) they successfully polarized ^7Li on ^7LiH (80 % at 0.2 K and 6.5 T) with a long build-up time (50 h) [23].

Table 2: Past records of irradiation conditions, obtained polarization and build-up time with their measurement conditions for ^7Li in ^7LiH . (α): The irradiation temperature was not well-defined; the target material was by 1 mm above the top of liquid argon level [21] [22].

Group	T_{Ir} (K)	E_e^- (MeV)	Dose $\times 10^{17}$ (e^-/cm^2)	$P_{^7\text{Li}}$ (%)	P_H (%)	T_{Build}	T(K)	B (Tesla)	Year Com- ments
Saclay [21] [22]	$\geq 87^{(\alpha)}$	3	3.7	40	60	100 h	0.6	5	1977
Saclay [23]	77	4	2	80	95	50 h	0.2	6.5	1978
Saclay [24]	150	300	2.5	10		24 h	0.2-0.4	2.5	1986
Saclay [25]	180	300	1	50	70	24 h	0.2-0.4	5	1988
		to 650	2	47	56	6 h	0.2-0.4	2.5	
LANL [26]	184	30	0.5	31	42	3 h	0.2-0.4	2.5	1992
PSI [27]	180	3	2	+46 -38		~ 2 -3 h to 20%	0.2-0.4	2.5	1992
Bonn [11]	180	20	1	12	42	50 m	1	2.5	1995 + $10^{15}e$ (1K)
				15		8 m	1	2.5	

Table 3: Past records by the Saclay [25] and the Bonn [11] groups for different irradiation temperatures and doses with obtained polarization and build-up time for ^7Li or H in ^7LiH at 0.2-0.4 K or 1 K and 2.5 T.

Group	T_{Ir} (K)	E_e^- (MeV)	Dose $\times 10^{17}$ (e^-/cm^2)	$P_{^7\text{Li}}$ (%)	P_H (%)	T_{Build}	T(K)	B (Tesla)	Year
Saclay [25]	180	300	1	25	35	10 h	0.2-0.4	2.5	1988
	180	to 650	2	47	56	6 h	0.2-0.4	2.5	
	180		3	44	58	11 h	0.2-0.4	2.5	
	190		1	30		3.5 h	0.2-0.4	2.5	
	190		2	-42	-52	10 h	0.2-0.4	2.5	
Bonn [11]	160	20	1		3.0		1	2.5	1995
	180		1		11	52 m	1	2.5	
	180		2		8.5		1	2.5	
	180		4		7.5		1	2.5	
	190		1		10		1	2.5	
	200		1		9.5		1	2.5	

The Saclay group tried the irradiation at 150 K with 2×10^{17} (e^-/cm^2) and obtained about 10 % of ^7Li polarization and about 24 h of build-up time [24]. Later, they started using variable higher temperatures and obtained shorter build-up time (6 h at 0.3 K and 2.5 T) at around 180 K [25] (see Table 2 and Table 3).

The LANL [26] and the PSI [27] groups obtained comparative polarizations and build-up times as the Saclay group did. The Bonn group [11] used 1 K instead of 0.3 K or 0.6 K reducing the build-up times (less than 1 h) with lower ^7Li polarizations (12 % at 2.5 T).

The Saclay and Bonn groups compared polarizations of ^7Li and H and their build-up times for different irradiation temperatures and doses as shown in Table 3. Both groups observed highest polarization for irradiation temperature of 180 K with doses of 2 (Saclay) and 1 (Bonn) $\times 10^{17}$ (e^-/cm^2) and reasonably short build-up time. If compare H polarizations and build-up time at 180 K and 1×10^{17} (e^-/cm^2) from these groups, they are 35 % (Saclay) and 11 % (Bonn), 10 h (Saclay) and 52 min (Bonn). They are very different and sensitive to the DNP temperatures (0.3 K (Saclay) and 1 K (Bonn)).

5.4 ^6Li and D polarizations in ^6LiD

Table 4: At six different irradiation temperatures with obtained polarization and build-up time for ^6Li in ^6LiD at 1 K and 2.5 T with dose of 10^{17} (e^-/cm^2) measured by the Bochum group [28].

Group	T_{Ir} (K)	E_e^- (MeV)	Dose $\times 10^{17}$ (e^-/cm^2)	$P_{^6\text{Li}}$ (%)	P_D (%)	T_{Build}	T(K)	B (Tesla)	Year
Bochum [28]	140	20	1.0	-3.7	-3.9	200 m	1	2.5	2001
	160		1.0	-3.1	-3.2	160 m	1	2.5	
	170		1.0	-6.3	-6.5	100 m	1	2.5	
	180		1.0	-11	-12	45 m	1	2.5	
	190		1.0	-14	-15	35 m	1	2.5	
	200		1.0	-13	-14	20 m	1	2.5	

The Bochum group studied with variable irradiation temperatures at 140 - 200 K, and obtained the highest polarization (-14 %) and reasonably short build-up time (35 min) [28] at 190 K as shown in Table 4.

For the variable doses shown in Table 5, the Bonn group observed higher D polarization for lower dose of 1×10^{17} (e^-/cm^2) than for 4×10^{17} (e^-/cm^2).

In the Table 5, the SLAC group reported comparable or slightly higher D polarization for dose of 3.7×10^{17} (e^-/cm^2) than for that of 2×10^{17} (e^-/cm^2).

As shown in Figure 10, the group shows deuteron polarization build-up behavior for ^6LiD target with different irradiation doses prior to E155 [12] and it is hard to obtain high polarization with too small (1.5×10^{17} (e^-/cm^2)) and large (4.5×10^{17} (e^-/cm^2)) doses in a reasonably short build-up time. It is not clear which dose is the better choice, 3.7×10^{17} (e^-/cm^2) or 2.0×10^{17}

(e^-/cm^2). The data shown in Figure 10 were taken with primary dose of 2.0×10^{17} (e^-/cm^2) during E155 experiments and show excellent radiation resistance performances.

Table 5: Three groups show ${}^6\text{Li}$ or D polarization and build-up time dependences on irradiation doses for ${}^6\text{LiD}$ target. Irradiation temperatures with best results are used for each group.

Group	T_{Ir} (K)	E_e^- (MeV)	Dose $\times 10^{17}$ (e^-/cm^2)	$P_{{}^6\text{Li}}$ (%)	P_D (%)	T_{Build}	T(K)	B (Tesla)	Year
Bonn [11]	180	20	1.0		12.0	46 m	1	2.5	1995
	180		4.0		6.0		1	2.5	
SLAC [12]	183	30	2		-23		1	5	1999
	183		3.7		-24		1	5	
Bochum [28]	190	20	0.1	-18	-19	220 m	1	2.5	2001
	190		0.2	-16	-16	160 m	1	2.5	
	190		1.0	-14	-15	35 m	1	2.5	

5.5 Options for irradiations

From the results in Sections 5.2, 5.3 and 5.4, optimal irradiation temperatures (180 to 190 K) and doses (1 to 3.7 K) are close for these three materials, ${}^7\text{LiD}$, ${}^7\text{LiH}$ and ${}^6\text{LiD}$. Possible options for ${}^7\text{LiH}$ and ${}^6\text{LiD}$ can be used to our ${}^7\text{LiD}$ targets by using the irradiation cryostat.

5.5.1 Post irradiations at low temperature

The Bonn group showed that additional dose of 1 % of 10^{17} (e^-/cm^2) at 1K to the main irradiation increased the ${}^7\text{Li}$ polarization in ${}^7\text{LiH}$ from 12 to 15 % and reduced the build-up time from 50 to 8 minutes [11] as shown at Table 2.

During RGC experiments, irradiations of an order of 1×10^{15} (e/cm^2) at around 1 K at Hall B beam line (11 GeV) were added to the primary irradiation to NH_3 and ND_3 targets, which improved polarizations significantly.

For RGG experiments, this low temperature additional irradiation is planned to ${}^7\text{LiD}$ material at irradiation cryostat setting to ~ 3 Kelvin and polarization and build-up time will be examined prior to the Hall B beam time.

5.5.2 Warm up target materials to room temperature after primary dose

As at Table 6, the Bochum group showed results for the irradiation temperatures at 140 to 190 K with dose of 1×10^{17} (e^-/cm^2) followed by holding the material at room temperature for ten minutes (from the second to fifth row). The first and sixth rows are without the above procedure. The highest polarization of -18 % and -19 % for ${}^6\text{Li}$ and D were observed for the sample with this procedure and irradiation at 140 K. For the sample of irradiation at 190 K, this procedure reduced polarization from -14 to -10, however the build-up time was shortened from 35 m to 20 m.

We plan to perform this optional procedure to ${}^7\text{LiD}$ target at 140 K.

Table 6: Records by the Bochum group for results with the warming up the samples up to room temperature for about ten minutes after irradiations for four different irradiation temperatures (from the second to fifth row and commented as "Warm RT"). The first and sixth rows show results without the procedure. Polarization for ^6Li and D in ^6LiD and build-up time are shown at 1 K and 2.5 T with dose of 10^{17} (e^-/cm^2).

Group	T_{Ir} (K)	E_e^- (MeV)	Dose $\times 10^{17}$ (e^-/cm^2)	$P_{^6\text{Li}}$ (%)	P_D (%)	T_{Build}	T(K)	B (Tesla)	Year Comments
Bochum [28]	140	20	1.0	- 4	- 4	200 m	1	2.5	
	140		1.0	-18	-19	60 m	1	2.5	Warm RT
	160		1.0	-14	-14	65 m	1	2.5	Warm RT
	180		1.0	-16	-17	60 m	1	2.5	Warm RT
	190		1.0	-10	-10	20 m	1	2.5	Warm RT
	190		1.0	-14	-15	35 m	1	2.5	

5.5.3 Lower dose

As shown at Table 5, the Bochum group observed higher ^6Li polarizations (-18 %) for 0.1×10^{17} (e^-/cm^2) than that (-14 %) for 1×10^{17} (e^-/cm^2), while the build-up time is about six times longer [28]. This low dose of 0.1×10^{17} (e^-/cm^2) may be an option to obtain higher polarization than with 1×10^{17} (e^-/cm^2) for ^7LiD sample. It might be useful to know for this low dose sample, how the build-up time can be reduced and polarization can change with additional irradiation dose of order of $\sim 10^{15}$ (e^-/cm^2) at 1 K.

5.6 Annealing

There are very limited annealing data only for ^6LiD (not for ^7LiD nor ^7LiH). The SLAC group annealed ^6LiD two times at 185 K for twenty minutes for samples whose post-doses reached 1×10^{16} (e^-/cm^2) during E155 experiments. After the anneal, the same maximum polarization as previously was attained. However, the rate of polarization decay with increasing charge was faster than before the anneal [12].

In our case, there might be options to anneal at higher temperature or to irradiate with a primary dose less than 1×10^{17} (e^-/cm^2) to check if there are changes of behaviors such as a lifetime of ^7LiD target material after anneal. The DNP polarizing cryostat allows us to compare results from these options.

During RGC experiments, NH_3 and ND_3 targets were annealed after a dose of about 4×10^{15} (e^-/cm^2) was accumulated to them (usually three day's of running) followed by another dose of accumulation with reversed polarization direction [15]. Since there are no data for radiation damages to ^7LiD targets, new data about their radiation resistance will be collected during the RGG experiments. If similar damages as to ^6LiD are expected, we may run for about six days without annealing them.

6. Summary

For the spin-dependent EMC effect experiment, JLab target and collaborating groups have been working for ^7LiD material production, setting up CEBAF injector beam line for the irradiation and designing and constructing irradiation and DNP polarize cryostats. From the past data shown at Section 5, with the irradiation temperature of 180 - 190 K and dose of $1 - 2 \times 10^{17}$ (e^-/cm^2), it is expected to obtain a ^7Li polarization of about 50 % and build-up time of a couple of hours for ^7LiD target. It is essential to obtain the best conditions (high polarization and short build-up time) prior to the scattering experiments by comparing behaviors of polarization and build-up time based on the standard temperature (180 - 190 K) and dose ($1 - 2 \times 10^{17}$ (e^-/cm^2)) and those with the following options. (1) irradiate at 140 K with dose of $1 - 2 \times 10^{17}$ (e^-/cm^2) and hold the sample at room temperature for 10 minutes after the irradiation. (2) add and optimize dose of order of 10^{15} (e^-/cm^2) to the sample of standard irradiation conditions described above with the irradiation cryostat at low temperature of ~ 3 K. (3) irradiate at 180 - 190 K with a dose smaller than 1×10^{17} (e^-/cm^2) and add post-irradiations of order of 10^{15} (e^-/cm^2). ESR and IR spectroscopy at DNP cryostat can lead to deeper understandings of mechanism of radiation damage, annealing and effects of optional irradiation procedures.

7. Acknowledgements

This material is based on works supported by the U.S. Department of Energy, Office of Science, Office of Nuclear Physics under contract DE-AC05-06OR23177 and the U.S. Department of Energy, Office of Science, Office of Fusion Energy Sciences under field work proposal JLAB-FES-2301.

References

- [1] Approved by Jefferson Lab PAC, *The EMC Effect in Spin Structure Functions* (E12-14-001)
- [2] J. Brock *et al.*, *A Solid Polarized Target Development Facility at Jefferson Lab*. (proceedings at this conference).
- [3] I. C. Clöet *et al.*, *EMC and polarized EMC effects in Nuclei*, Phys. Lett. B642 (2006) 210..
- [4] U. Landgraf (NMC Collaboration.), *Nuclear Effects in Deep Inelastic Scattering*, Nucl. Phys. A527 (1991) 123C.
- [5] J. Arrington *et al.*, *Measurement of the EMC effect in light and heavy nuclei* Phys. Rev. C 104 (2021) 065203.
- [6] J. Gomez *et al.*, *Measurement of the A dependence of deep-inelastic electron scattering*, Phys. Rev. D 49 (1994) 4348.
- [7] B.S. Pudliner *et al.*, *Quantum Monte Carlo calculations of nuclei with $A \leq 7$* , Phys. Rev. C 56 (1997) 1720.
- [8] S. Cohen and D. Kurath, *Effective interactions for the 1p shell*, Nucl. Phys. 73 (1965) 1.

- [9] R.B. Wiringa *et al.*, *Nucleon and nucleon-pair momentum distributions in $A \leq 12$ nuclei*, Phys. Rev. C 89 (2014) 024305.
- [10] B. van den Brandt *et al.*, *Results from the PSI ^6LiD Target*, in: Proc. of 9th Int. Symposium of High Energy Spin Physics, 1990, 320.
- [11] S. Goertz *et al.*, *Investigations in high temperature irradiated $^6/7\text{LiH}$ and ^6LiD , its dynamic nuclear polarization and radiation resistance*, Nuclear Instruments and Methods in Physics Research A 356 (1995) 20.
- [12] S. Bueltmann *et al.*, *A study of lithium deuteride as a material for a polarized target*, Nuclear Instruments and Methods in Physics Research A 425 (1999) 23.
- [13] J. Ball *et al.*, *First results of the large COMPASS ^6LiD polarized target*, Nuclear Instruments and Methods in Physics Research A 498 (2003) 101.
- [14] S. Pisano *et al.*, *Single and double spin asymmetries for deeply virtual Compton scattering measured with CLAS and a longitudinally polarized proton target*, Phys. Rev. D91 (2015) 052014.
- [15] P. Pandey *et al.*, *Operation of a Longitudinally Polarized Solid Nuclear Target in CLAS12*, in: Proc. of 25th Int. Symposium of Spin Physics. 2023, 211.
P. Pandey, *Longitudinal Solid Polarized Target for CLAS12 and Study of Spin Structure of Nucleons*, Doctor of Philosophy (PhD), Dissertation, Physics, Old Dominion University, 2024, DOI: 10.25777/jmae-c846.
- [16] J. Brock, *1 K refrigerator for the CLAS12 Polarized Target Design, Construction, and First Results*, 18th International Workshop on Polarized Sources, Targets, and Polarimetry, 2019, 056.
- [17] C. Keith *et al.*, *First Use of a Longitudinally Polarized Target with CLAS12*, in: Proc. of 19th Workshop on Polarized Sources, Targets and Polarimetry, 2022, 009.
- [18] J. Maxwell, *NMR Measurements for Solid Polarized Targets at Jefferson Lab*, In: Proc. of 23rd International Symposium on Spin Physics, (2018) 102.
- [19] From the web-site of Cambridge Isotope Laboratories, Inc and exchanging emails answering to our questions.
- [20] C.G. Bustillos *et al.*, *Densification and microstructure features of lithium hydride fabrication*, Annals of Nuclear Energy 185 (2023) 109709.
- [21] Y. Roinel and V. Bouffard, *Polarisation dynamique nucléaire dans l'hydrure de lithium*, Journal de Physique 38 (1977) 817.
- [22] J. Ball, *Thirty years of research with lithium compounds in Saclay*, Nuclear Instruments and Methods in Physics Research A 526 (2004) 7.

- [23] A. Abragam, *Polarized targets in high energy and elsewhere*, in: Proceedings on 3rd International Symposium on High Energy Physics with Polarized Beams and Polarized Targets (1978) 1.
- [24] P. Chaumette *et al.*, *Progress report on polarization of ^6LiD and ^7LiH irradiated with high energy electrons*, Helvetica Physica Acta, 58 (1986) 767.
- [25] P. Chaumette *et al.*, *Progress report on polarization of irradiated ^6LiD and ^7LiH* , in: Proc. of 8th Int. Symposium of High Energy Spin Physics. 1988, 1275.
- [26] J.J. Jarmer *et al.*, *Polarization of Irradiated Lithium Hydride*, in: Proc. of 10th International Symposium on High Energy Spin Physics, 1992, 363.
- [27] B. van den Brandt *et al.*, *Operation of a Polarized ^7LiH Target*, in: Proc. of 10th Int. Symposium of High Energy Spin Physics, 1992, 369.
- [28] A. Meier, *^6LiD for the polarized target of the COMPASS experiment*, PhD. Thesis, Ruhr-University Bochum 2001.